Effects of Coulomb interaction on the electronic structure and lattice dynamics of the Mott insulator Fe_2SiO_4 spinel

Mariana Derzsi*
Institute of Nuclear Physics, Polish Academy of Sciences, Radzikowskiego 152, PL-31342 Kraków, Poland and Department of Theoretical Chemistry, Institute of Inorganic Chemistry, Slovak Academy of Sciences, Dúbravská cesta 9, SK-84536 Bratislava, Slovakia

Przemysław Piekarz, Paweł T. Jochym, Jan Łażewski, Małgorzata Sternik, Andrzej M. Oleś, and Krzysztof Parlinski
Institute of Nuclear Physics, Polish Academy of Sciences, Radzikowskiego 152, PL-31342 Kraków, Poland
(Received 30 January 2009; revised manuscript received 3 April 2009; published 8 May 2009)

Using the *ab initio* density-functional generalized gradient approximation with varying on-site Coulomb interaction U, the electronic and crystal structures of Fe_2SiO_4 spinel were optimized at high pressure. It was found that the ground state changes from the metallic ferromagnetic state at $U=0$ into the antiferromagnetic state, stable in the regime of Mott insulating state for $U>2$ eV. We found that Fe_2SiO_4 spinel is an antiferromagnetic Mott insulator at the realistic value of $U\sim4.5$ eV, with a distinct gap which opens in the minority-Fe($3d$) states. We point out that the low value of the Néel temperature $T_N\sim12$ K follows from the geometrical frustration of magnetic interactions, while the exchange constant $J\sim1.7$ meV estimated from the energies of ordered magnetic phases gives a rather high value of the Curie-Weiss temperature $\theta_{CW}\simeq340$ K. The phonon-dispersion curves and phonon density of states were derived for both the metallic and insulating antiferromagnetic phase of Fe_2SiO_4 spinel, and significant changes of energy and dispersion of certain phonon modes, particularly with large Fe character, caused by local electron correlations were detected and analyzed. We point out some similarities with the electronic and dynamical properties of magnetite.

DOI: 10.1103/PhysRevB.79.205105 PACS number(s): 71.27.+a

I. INTRODUCTION

Fe_2SiO_4 is Fe-end member of geologically and geophysically very important mineral $(Mg,Fe)_2SiO_4$. As the most abundant mineral in the Earth upper mantle, it is believed to have dominant influence on crucial geophysical processes in this part of the Earth such as thermodynamics of rock-forming minerals and mechanisms that drive plate tectonics. Detailed characterization of this mineral and its end members, Mg_2SiO_4 and Fe_2SiO_4, is, therefore, crucial for future understanding of the main Earth processes. $(Mg,Fe)_2SiO_4$ is known to exists in three phases: (i) low-pressure α orthorhombic (olivine), (ii) moderate-pressure β orthorhombic (wadslayite), and (iii) high-pressure γ cubic (ringwoodite).[1] So far, several experimental[2] and theoretical[3] studies have been reported concerning the structural, dynamical, and thermodynamical properties of Mg_2SiO_4, crystallizing in all three $\{\alpha,\beta,\gamma\}$ phases.

Fe_2SiO_4 with its only two stable phases (α fayalite and γ spinel) represents much more challenging material as it belongs to the group of transition metal orthosilicates, additionally possessing nonvanishing magnetic moment. In these materials strong local Coulomb interactions play a very important role, and are responsible for the observed ground states and low-energy excited states which determine their low-temperature properties. The electronic interactions suppress charge fluctuations in Mott insulators, and lead to rather strong coupling between spin, charge, orbital, and lattice degrees of freedom,[4] so the standard density-functional theory (DFT) often fails and does not reproduce the observed electronic structure and magnetic properties. And indeed, the failure of the standard DFT was recently demonstrated also in case of the Fe_2SiO_4 fayalite. Its structural, electronic, and magnetic properties have been studied using the well-established local density approximation and generalized gradient approximation (GGA).[5] Although sufficient to reproduce the crystal structure and simplified collinear antiferromagnetic (AF) spin order, they failed to reproduce the electronic structure of a Mott insulator, describing it instead as a band metal. Only after the inclusion of strong on-site Coulomb interactions between the $3d$ electrons within the GGA+U approach (with the realistic value of $U=4.5$ eV), the correct AF-insulating state was reproduced.[6] Fe_2SiO_4 fayalite is known as a Mott-Hubbard insulator[7] and its magnetic structure was proved to be quite complex. The λ-type phase transition of fayalite is observed at temperature equal to its Néel temperature $T_N=64.9$ K.[8] Below T_N, the ordered state corresponds to a noncollinear AF phase with a strong magnetocrystalline anisotropy. These experimental findings are a clear manifestation of strong interrelation between the crystal, electronic, and magnetic properties.

In comparison to the Fe_2SiO_4 fayalite, its high-pressure γ spinel phase is a much less studied system. Its Mössbauer spectra obtained at room temperature and pressures in the range 0–16 GPa exhibit a quadrupole doublet, being a characteristic feature of the paramagnetic state.[9] Although, there are some experimental indications of the AF order at low temperatures [a phase transition similar to fayalite has been observed in the spinel structure at much lower temperature $T_N=11.8$ K (Ref. 10)], the accurate magnetic as well as the electronic structure of the spinel is not yet known. To our best knowledge no theoretical DFT calculations have been performed for the spinel phase of Fe_2SiO_4 until now.

Transition metal compounds crystallizing in the spinel structure exhibit, apart from the strong correlations between

magnetic, structural, and dynamical properties, another very interesting effect, namely, appearance of highly frustrated spin ground state due to special crystal geometry (pyrochlore lattice).[11] Usually in such systems no long-range order occurs, and a disordered spin state (spin ice) is observed up to very low temperatures.[12] Additionally, the coupling between the spin and lattice degrees of freedom (spin-phonon coupling) leads to such phenomena such as the renormalization of the phonon frequencies and induces changes in magnetic excitation spectrum. A strong spin-phonon coupling has been observed in the $ZnCr_2O_4$ spinel, where the AF order induces the tetragonal deformation and large phonon splitting below the Néel temperature.[13] As found in recent studies,[14] the interplay of electron interactions with phonons in presence of local electron correlations plays an important role also in the mechanism of the Verwey phase transition in magnetite (Fe_3O_4). Interestingly, Fe_2SiO_4 spinel differs from magnetite only by the atom type at the tetrahedral site (Si instead of Fe), not active in the Verwey transition, so one expects that the comparison of the electronic and dynamical properties of these two compounds could shed some light on the cooperative character of phenomena in both systems near the metal-insulator transition.

At the metal-insulator transition the changes in the electronic structure and electron localization with increasing local (on-site) Coulomb interaction U induce drastic modification of the electron-phonon interaction and screening properties, so strong changes in the phonon spectra may be expected. Such anomalies have been observed for instance in the high-T_c superconductors, where strong phonon softening occurs when the Mott insulating state is doped.[15] The effect of the local Coulomb interactions on phonon spectra in transition metal oxides was studied using either the dynamical mean-field theory,[16] or the LDA+U approach.[17,18] Recently, dependence of phonon frequencies on U was found for the olivine mineral Ni_2SiO_4 using the GGA+U studies.[19]

In this paper, we analyze the electronic, magnetic, and structural properties in the ground state of Fe_2SiO_4 spinel (at temperature $T=0$) as a function of the on-site Coulomb interaction parameter U within the GGA+U approach. Next, by calculating the phonon energy spectrum, the interrelation between the electronic structure and lattice dynamics is studied. The paper is organized as follows. The calculation methods are given in Sec. II. In Sec. III A, the crystal structure properties and possible magnetic orders are discussed. Section III B describes the electronic structure and Sec. III C magnetic interactions. The phonon-dispersion curves and phonon density of states (total and projected on individual atoms) are presented in Sec. III D. In Sec. IV we compare the properties of the present spinel compound with those of magnetite and highlight the consequences of strong Coulomb interactions. The paper is summarized in Sec. V.

II. CALCULATION METHODS

Spin polarized calculations were performed using the Vienna *ab initio* Simulation Package (VASP) (Ref. 20) based on the DFT approach which makes use of the Perdew, Burke, and Ernzerhof (PBE) functional[21] applying the projector augmented wave method with GGA-PBE potentials. The model structures were fully optimized (atomic positions and lattice constants) at hydrostatic pressure equal to 20 GPa. The wave functions were expanded in-plane waves up to the kinetic-energy cutoff of 500 eV. The Monkhorst-Pack **k**-point generation scheme was used with a grid of $4\times4\times4$ points in the irreducible Brillouin zone. All calculations were performed in the $1\times1\times1$ supercell with 56 atoms. The electronic and ionic optimizations were continued until the energy differences between the successive electronic and ion cycles were less than 10^{-7} and 10^{-5} eV, respectively. Both standard GGA calculations and GGA+U calculations were performed. In order to take into account the on-site Coulomb interactions between $3d$ electrons,[22] the values of the Coulomb integral $U=4.5$ eV eV (following Ref. 5) and Hund's exchange $J_H=0.90$ eV (estimated from the Racah parameters B and C given in Ref. 23) were used for Fe^{2+} ions in Fe_2SiO_4 in the spin-polarized GGA+U calculations.

The phonon frequencies were determined for the considered magnetic state of Fe_2SiO_4 spinel using the direct method,[24] implemented in the PHONON software.[25] For the phonon calculations, the forces at individual atoms had to be minimized. The optimization process was stopped when all the forces on the individual atoms were lower than 10^{-5} eV/Å (the maximal obtained force on each atom was 7×10^{-6} eV/Å). The force constants matrix elements were derived from the Hellmann-Feynman (HF) forces calculated by displacing single (nonequivalent) atoms from their equilibrium positions by $u=0.02$ Å. By the diagonalization of the dynamical matrix, the phonon frequencies and polarization vectors were obtained. For $U=4.5$ eV, the electronic state is insulating, so the long-range polarization effects on phonon energies have to be taken into account. To estimate the transverse-longitudinal (LO-TO) splitting at the Γ point, we used the nonanalytical formula for the energy of the LO mode at $k\rightarrow0$.[26] The effective charges are approximated by the nominal (ionic) values: $Z^*(\mathrm{Fe})=2$, $\vec{Z}^*(\mathrm{Si})=4$, and $Z^*(\mathrm{O})=-2$, and the static dielectric constant $\varepsilon=3.5$ was taken from the experimental optical measurements for fayalite.[27]

III. RESULTS AND DISCUSSION

A. Crystal structure

It is known that Fe_2SiO_4 spinel has a cubic symmetry crystallizing in $Fd\bar{3}m$ space group. Synthesized from fayalite at pressure $p=75$ kbar and temperature $T=1500$ K, the cell size of $a=8.234(1)$ Å was determined from the powder x-ray diffraction refinement.[28] The unit cell contains 8 f.u. with 56 atoms: 32 oxygen, 16 iron, and 8 silicon atoms. The oxygen atoms have an approximate fcc arrangement, the silicon atoms are tetrahedrally coordinated by oxygen atoms and the iron atoms occupy the centers of oxygen octahedra. In each crystallographic plane (ab, bc, and ac), the Fe atoms are organized into chains, running parallel to the diagonal of the respective plane. The chains in the successive planes (e.g., ab planes) are oriented perpendicularly to each other, allowing for the existence of the Fe tetrahedra. Figure 1 shows the crystal structure from the perspective of the Fe chains formed in the ab planes.

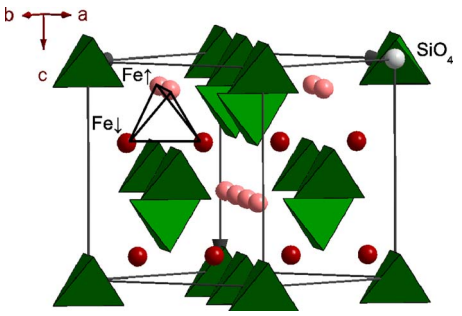

FIG. 1. (Color online) Crystal structure of Fe_2SiO_4 spinel. Lines show the unit cell edges, the unit cell contains SiO_4 tetrahedra and chained structures of Fe atoms which form in the *ab* planes. In the AF phase, the dark and light (red) atoms represent iron atoms with spin down (Fe↓) and up (Fe↑), respectively. The Fe atoms are additionally organized into tetrahedra, sharing all four edges. The surfaces of the Fe tetrahedra are equal armed triangles. In case of AF order, these triangles are formed between two Fe atoms with the same spins and one with opposite spin, i.e., 2Fe↑ and 1Fe↓ or 2Fe↓ and 1Fe↑. One such Fe tetrahedron and the crystallographic axes *a*, *b*, and *c* are shown in upper left corner.

Due to large Hund's exchange element J_H, the Fe^{2+} ions with electronic configurations close to $3d^6$ carry large magnetic moments. However, the low-temperature magnetic state is not known—therefore we have examined both, the ferromagnetic (FM) and AF configuration of the magnetic moments on Fe atoms. Setting parallel magnetic moments on all Fe atoms in the *ab* plane and antiparallel in the planes alternating along the *c* direction, we have constructed the AF order along the Fe chains lying in the *ac* and *bc* planes (see Fig. 1). Therefore, in the AF state one-bond direction (e.g., the one along *c* axis) becomes distinct and the symmetry of the crystal is lowered. In fact, the onset of AF order reduces the original cubic (fcc) symmetry to the tetragonal bct symmetry $I4_1/amd$. This distortion is very small when applying the GGA approach (~0.04%), in which local Coulomb interactions are neglected. However, it becomes significantly amplified (to 1.00%–1.44%) when the on-site Coulomb interaction parameter U is introduced and its values in the realistic range of $2<U<5.5$ eV are considered.

With increasing value of U, the deformation of the cubic symmetry is accompanied by the expansion of the structure in the *ab* plane and its compression along the *c* axis, while its volume simultaneously increases (see Table I). The volume increase found with increasing U is typical for the GGA $+U$ calculations,[29] and it is, therefore, observed here for both the FM and the AF phase. However, there is a qualitative difference in the behavior of the volume for these two magnetic model structures. While the lattice constants and the volume of the AF structure change smoothly with U, a sudden jump was observed for both of them in case of the FM structure between $U=2.0$ and $U=3.0$ eV, see Figs. 2(a) and 2(b). Within this range, the unit cell volume in the FM structure rises abruptly up to a value slightly above the AF one, and the next follows the AF volume rather closely for larger values of U. In the range of $U>3.0$ eV, the unit cell vol-

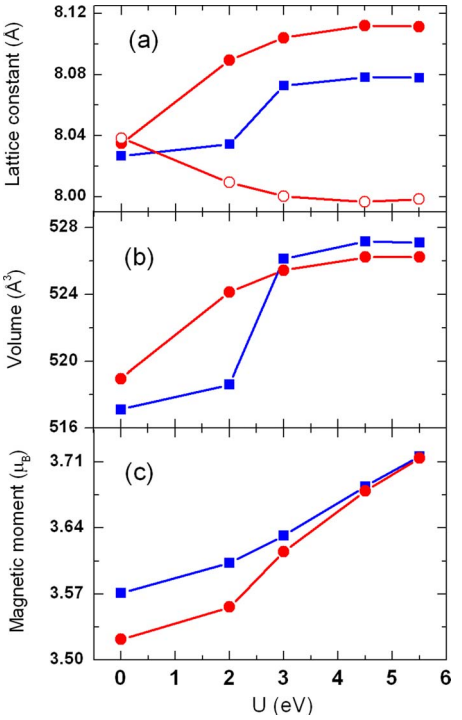

FIG. 2. (Color online) Dependence of structural and magnetic properties on the Coulomb element U: (a) lattice constants, (b) unit cell volume, and (c) magnetic moments. For $U\geq 2$ eV, we assume a constant value of $J_H=0.9$ eV (except for $U=J_H=0$). In all cases the results obtained for the FM (squares) and AF (circles) phase are compared. In case of the AF structure, the lattice constants $a=b$ are shown by full circles and *c* by open circles in panel (a).

TABLE I. Comparison of the structural parameters *a*, *c* (Å), unit cell volume *V* (Å^3), enthalpy $H=E+pV$ (eV), and magnetic moment μ (in μ_B) as a function of *U* (eV) for the FM and AF structures. For the AF configuration, the cell parameter *c* is also shown, since its unit cell has tetragonal $I4_1/amd$ symmetry.

	Ferromagnetic				Antiferromagnetic				
U	*a*	*V*	*H*	μ	*a*	*c*	*V*	*H*	μ
0.0	8.0266	517.124	−363.222	3.571	8.0350	8.0383	518.963	−360.213	3.522
2.0	8.0343	518.614	−354.679	3.603	8.0895	8.0094	524.135	−354.672	3.556
3.0	8.0729	526.125	−348.920	3.632	8.1041	8.0004	525.438	−349.140	3.615
4.5	8.0783	527.181	−343.130	3.684	8.1120	7.9968	526.222	−343.468	3.679
5.5	8.0779	527.103	−339.969	3.716	8.1113	7.9984	526.240	−340.305	3.714

umes for both magnetic structures show similar behavior with increasing U, changing very slowly, while the change itself has a decreasing tendency. The values of the FM and AF lattice constants are reaching their saturation near $U=4.5$ eV, and a higher value of U has practically no influence on the crystal structure of Fe_2SiO_4 spinel. This suggests that the localization of $3d$ electrons due to rather strong electron interactions is almost complete and the system is in strongly correlated regime.

The distortion of the cubic symmetry, caused by the AF order, influences also the interatomic distances. In the present structure the distances between the nearest-neighbor Fe ions, which form triangular sublattices (Fe tetrahedra) with equivalent arms, see Fig. 1, may be influenced by electron correlations. Indeed, one finds that the respective Fe-Fe distances increase with U for both magnetic structures. Additionally, as the AF structure contracts along the c direction and expands in the ab plane, the Fe tetrahedra get distorted—two of their sides are being shortened and the remaining two are being elongated. In other words, those Fe-Fe distances which connect the atoms of the same spin increase and the ones connecting the atoms carrying opposite spins decrease as the structure deforms, i.e., $d(\mathrm{Fe}\uparrow\text{-}\mathrm{Fe}\downarrow) < d(\mathrm{Fe}\uparrow\text{-}\mathrm{Fe}\uparrow)$. These changes are very small when applying the GGA approach, but increase and become significant when realistic on-site Coulomb interactions are considered. Using $U=4.5$ eV, we obtained 2.868 and 2.848 Å, for $d(\mathrm{Fe}\uparrow\text{-}\mathrm{Fe}\uparrow)$ and $d(\mathrm{Fe}\uparrow\text{-}\mathrm{Fe}\downarrow)$ distances, respectively. Interestingly, the average of the two values equals the Fe-Fe distance found for the FM structure at the same value of U: $d(\mathrm{Fe\text{-}Fe})_{\mathrm{AF}}=d(\mathrm{Fe\text{-}Fe})_{\mathrm{FM}}=2.858$ Å. This relation between the Fe-Fe distances in the AF and FM structures was found to be nearly independent of U.

For both magnetic states, the magnetic moment increases with U [Fig. 2(c)], which effectively enhances the exchange splitting (see Sec. III B). The magnetic moment is larger for the FM structure when $U<3$ eV, which may be understood as certain moment amplification due to larger kinetic energy of $3d$ electrons in the FM phase. This difference is gradually lost above the metal-insulator transition when electrons localize in both magnetic structures.

Concerning the energetic stability of the two magnetic states, the GGA approach favors considerably the FM over the AF configuration by as much as 50 meV/atom. Including the U parameter, the two magnetic states become energetically close to each other already at $U=2$ eV, and for $U>2$ eV the AF state is more stable. A very small enthalpy difference between the AF and FM states, $\Delta H=6$ meV/atom for larger values of U, including the expected value $U=4.5$ eV, shows that these two states are almost degenerate and the AF interactions are rather weak. Table I summarizes the lattice parameters a and c, unit cell volumes V, total enthalpies H, and magnetic moments μ calculated as a function of the on-site Coulomb parameter U for the two magnetic structures, with either FM or AF order. As will be discussed in the Sec. III B, the main qualitative change in the crystal structure and the magnetic ground state, which occurs in the range of $2<U<3$ eV, is associated with the metal-insulator transition. The increase in the lattice parameter a and the volume V is smooth in the AF phase, as in this case

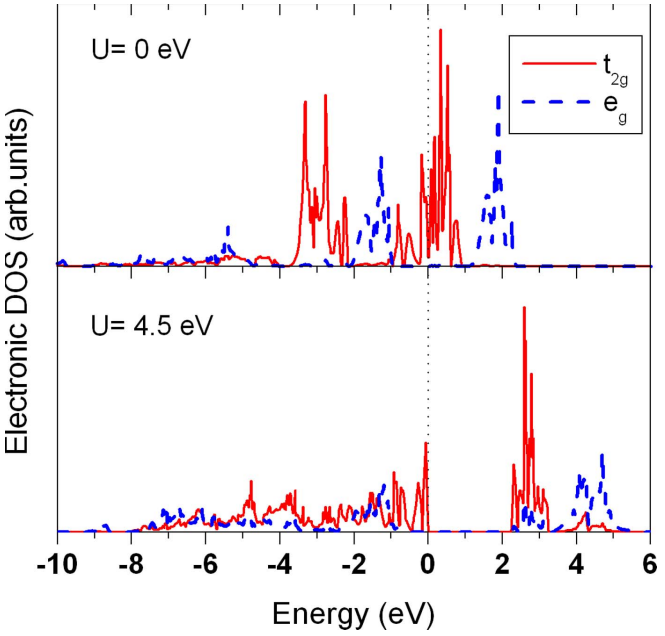

FIG. 3. (Color online) The electronic DOS for $3d$ orbitals obtained for the AF structure for $U=0$ eV (top) and 4.5 eV (bottom). Partial DOS for the t_{2g} and e_g states is shown by full and dashed line, respectively. In the FM structure a similar splitting of the $3d$ orbitals occurs for $U=4.5$ eV.

electron localization is gradual, in contrast to the FM phase.

B. Electronic structure

In this section, we analyze the electronic structure of Fe_2SiO_4 spinel as a function of increasing Coulomb interaction U. It was found, that both FM and AF states behave as metals for $U\leq 2$ eV, and as insulators for $U\geq 3$ eV. In the metallic regime, the finite density of states (DOS) around the Fermi level originates entirely from the Fe($3d$) orbitals. For $U=0$, the region of $3d$ states is about 6 eV wide and extends from −4 eV below the Fermi level up to about 2 eV above it (see Fig. 3, top). It is formed out of four distinct bands, shaped by crystal-field and exchange interactions.

The crystal field in the iron-centered oxygen FeO_6 octahedra is responsible for the splitting of $3d$ orbitals into two groups of states: three lower t_{2g} states and two higher e_g states by amount equal to E_{CF} (small deformations of the octahedra contribute only little to this splitting). Both groups split further (by E_{EX}) into two subgroups of spin-up and spin-down states because of the local exchange interaction which stabilizes high-spin states at Fe^{2+} ions. The above described splitting is schematically visualized in Fig. 4. Due to large Hund's exchange interaction, all five lower $3d$ states (t_{2g} and e_g) are occupied by electrons with majority spins, and only one higher t_{2g} state is occupied by opposite (minority) spin. The Fermi level crosses the upper energy minority-spin t_{2g} states in the metallic state at $U=0$.

The electronic structure changes qualitatively at $U>2$ eV, and a gap opens at the Fermi level, as shown in Fig. 5. By comparing the two partial DOSs in Fig. 3, it is evident that the gap opening results from the splitting of the

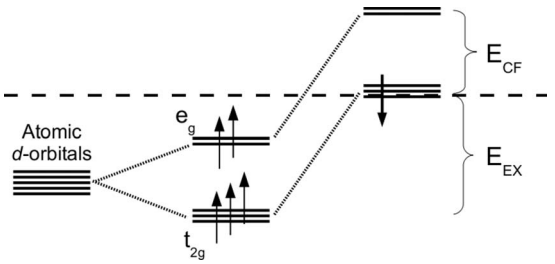

FIG. 4. Schematic splitting of the atomic Fe(3*d*) orbitals in Fe_2SiO_4 crystal. E_{EX} represents the splitting due to exchange interactions and E_{CF} shows the crystal-field splitting. Dashed line indicates the position of the Fermi level.

minority-t_{2g} states at the Fermi level. This splitting removes the degeneracy of t_{2g} orbitals and orbital order could occur. The opening of the gap shows that both magnetic structures become insulating already in the range of relatively weak Coulomb interaction $U \sim 2.5$ eV, well below the realistic value. This observation confirms our interpretation that Fe_2SiO_4 spinel is a Mott insulator.

The metal-insulator transition may be interpreted as follows. The analysis of the electron-density distribution in 3*d* orbitals performed for $U=0$ eV (Fig. 3, top) demonstrates that the width of the t_{2g} band crossing the Fermi level is approximately 2 eV. Therefore, one may argue qualitatively that when $U>2$ eV, electrons in the minority-t_{2g} states do not gain sufficient kinetic energy in the metallic state to overcome the Coulomb repulsion U. As a result, they become localized and a gap in the electronic structure opens. This mechanism of gap opening, as well as the close to linear increase in the electronic gap with U (Fig. 5), is typical for the Mott-Hubbard insulators.[30] Since the value of the insulating gap in Fe_2SiO_4 spinel has not been measured yet, the direct confirmation of our result is not possible at the moment. In comparison to fayalite, for which the insulating gap $\Delta=0.92$ eV calculated for the AF phase,[6] with $U=4.5$ eV and $p=25.4$ kbar, correlates well with the experimental values of 0.99 (Ref. 31) and 1.12 eV (Ref. 32), our calculations predict a two times higher value of the gap for the spinel phase.

As expected from a higher kinetic energy and weaker electron localization in FM states, the metal-insulator transition occurs first in the AF phase, and the transition in the FM phase follows for a somewhat larger value of U. Therefore, for each value of U within the insulating phase, a smaller electronic gap was obtained in the FM phase than in the AF one. This is particularly pronounced near the metal-insulator transition—for instance, for $U=3$ eV the width of the FM gap reaches only ~23% of the value obtained for the AF phase. For higher values of U, the difference between the FM and AF gap is almost constant, being ~0.7 eV, so for $U=5.5$ eV one finds that the FM gap is already at ~78% of the respective AF gap.

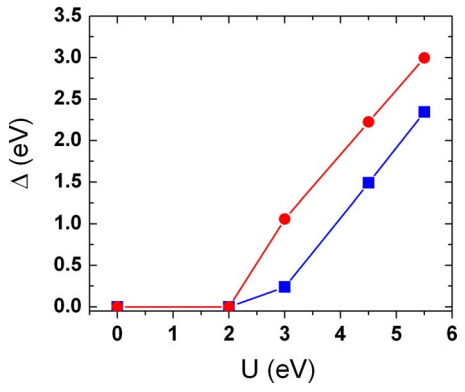

FIG. 5. (Color online) The insulating gap Δ in the electronic structure as a function of U, obtained for FM (squares) and AF (circles) phases.

Note that the exchange splitting raises when a finite value of U accompanied by $J_H=0.9$ eV is used (not shown). Local interactions contribute to it solely with Hund's exchange $\propto J_H$ in the present approach,[33] and this increase does not suffice to open a gap in the electronic structure at $U=2$ eV. This result shows that the exchange splitting alone does not contribute to electron localization which occurs at a stronger local Coulomb interaction U, where the gap Δ opens. The transition to the insulating state influences only weakly the magnetic state, and the magnetic moment increases stronger in the AF phase [Fig. 2(c)]. When U increases beyond $U=3$ eV, a further weak increase in the magnetic moments μ is found in both magnetic phases (see Table I). Thereby the values of the magnetic moments in the FM and AF phase gradually approach each other when U increases in the insulating regime, as the localization of t_{2g} electrons which decides about the local magnetic moments[33] is similar in both phases in the regime of large $U>4.5$ eV.

C. Magnetic interactions

The interactions responsible for the magnetic ground state of Fe_2SiO_4 spinel can be theoretically estimated by calculating the interatomic-exchange constant J, by making use of the total energies in the ordered FM and AF structures, E_{FM} and E_{AF}. Considering the Heisenberg model, we write the classical expression for the magnetic energy $E_J=J\Sigma_{ij}\mathbf{S}_i\mathbf{S}_j$, where $J>0$ for the expected AF structure and $\mathbf{S}_i$ is the magnitude of total spin at the Fe atom i, the total energy of the system per Fe atom is given by

$$E_\alpha = E_0 + E_J^\alpha. \quad (1)$$

Here E_0 is the energy of the nonmagnetic state and α denotes FM or AF phase. We derived the value of J from the energy difference between both magnetic phases following from Eq. (1), i.e., from $\Delta E=E_J^{FM}-E_J^{AF}$. While calculating E_J^α energies, we assume that all nearest-neighbor (NN) magnetic moments (spins) interact via the same exchange constant J and we take into account only the NN interactions. Here, we neglect small changes in J resulting from the tetragonal distortion. Then, each magnetic moment interacts with six spins ($z=6$) at the nearest-neighbor Fe sites as can be seen in Fig. 6, and each bond $\langle ij\rangle$ contributes for the atoms i and j. In the AF state, there are four bonds with antiparallel spins and two with parallel ones in a single tetrahedron (indicated by dashed and full lines in Fig. 6), so $E_J^{AF}=-JS^2$, with $J>0$ and S standing for the average spin. In the FM state, all bonds connect parallel spins, so $E_J^{FM}=3JS^2$. Using these values, one

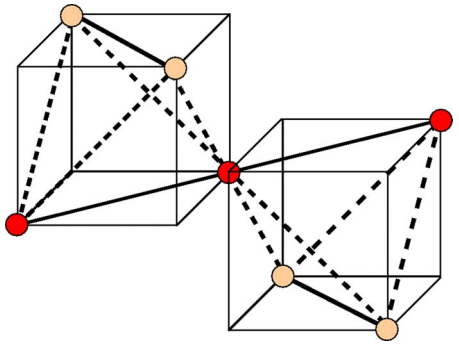

FIG. 6. (Color online) Schematic representation of nearest-neighbor Fe-Fe spin interactions between Fe atoms in the AF ordered structure with spin up and spin down indicated by light and dark circles, respectively. Focusing at the Fe atom common for both cubes, it is clear that it is involved in NN spin interactions along six bonds. Dashed lines represent the AF bonds and full lines represent the FM bonds.

finds the difference in total energies $\Delta E=4JS^2$.

Due to large Hund's (intra-atomic) exchange interaction $J_H=0.9$ eV, five out of six Fe($3d$) electrons occupy states with majority spins and only one occupies the minority-spin state (Fig. 4). Therefore, the total magnetic moment on single Fe atom is close to $4\mu_B$ (see Table I) which gives the total spin on a Fe atom $S=2$. Taking $S=2$, we obtain $J=1.72$ meV for $U=4.5$ eV. Using the mean-field formula for the Curie-Weiss temperature,

$$k_B\theta_{\mathrm{CW}}=\frac{1}{3}JzS(S+1), \tag{2}$$

where k_B is the Boltzmann constant, we estimate that $\theta_{\mathrm{CW}}=340$ K, which is much higher than the Néel temperature $T_N=11.8$ K observed in Fe_2SiO_4 spinel. Hence, we predict that future measurements of the magnetic susceptibility would give the Curie-Weiss law over a broad temperature regime.

The above large difference between T_N and θ_{CW} indicates strongly frustrated magnetic ground state, and has been observed also in similar systems, for instance, in $ZnCr_2O_4$.[13] The frustration arises here from the conflict between the spinel crystal structure and the exchange interaction $J>0$ which favors AF spin order; see Fig. 6. Considering the AF model structure, the tetragonal arrangement of Fe atoms does not allow for all NN spin interactions to become AF, and simultaneous minimization of the interaction energies for the bonds extending from a given site is forbidden. Therefore, the magnetic structure becomes frustrated, and can arise only below a rather low $T_N=11.8$ K.

D. Lattice dynamics

To complete information about the properties of Fe_2SiO_4 spinel, we present below a study of the lattice dynamics for the AF configuration, which corresponds to the ground state for realistic Coulomb interactions. We shall discuss the effect of U on the phonon spectra by comparing the results for $U=0$ and $U=4.5$ eV. The phonon spectrum of the Fe_2SiO_4 spinel in the cubic symmetry consists of 42 modes (Fig. 7). We performed the group theory analysis which allows us to conclude that the 39 optical modes form the following irreducible representations at the Brillouin zone center,

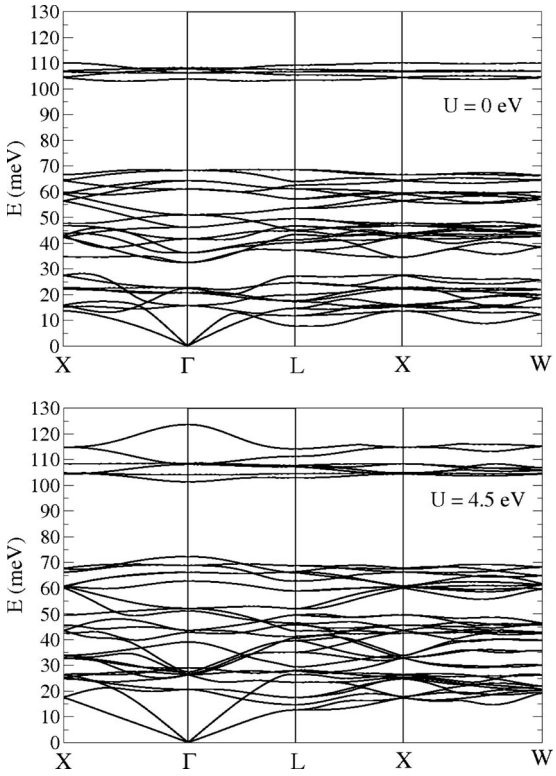

FIG. 7. Comparison of the phonon-dispersion curves calculated for the AF structure of Fe_2SiO_4 spinel with $U=0$ (top) and $U=4.5$ eV (bottom). The high symmetry points from left to right in units of $\frac{2\pi}{a}$ are: $X=(1,0,0)$, $\Gamma=(0,0,0)$, $L=(\frac{1}{2},\frac{1}{2},\frac{1}{2})$, and $W=(1,\frac{1}{2},0)$.

$$\Gamma_{\mathrm{op}}=A_{1g}+2A_{2u}+2E_u+E_g+4T_{1u}+2T_{2u}+T_{1g}+3T_{2g}, \tag{3}$$

where A_{1g}, E_g, and T_{2g} modes are Raman active, T_{1u} modes are infrared active, and A_{2u}, E_u, T_{2u}, and T_{1g} are silent (inactive). In agreement with the dimension of these representations, all E modes are doubly degenerate and all T modes are triply degenerate at the Γ point.

The phonon spectrum calculated for Fe_2SiO_4 spinel with $U=0$ eV (Fig. 7, top) is characterized by three separate energy regions 0–30, 31–70, and 103–118 meV. Modes in the two lower energy windows show considerably larger dispersion than modes arising in the highest energy one. The acoustic modes are found only in the lowest-energy region. The three separate energy regions are clearly visible in the total DOS in Fig. 8(a).

The origin of different phonon modes becomes evident by analyzing partial DOS calculated for individual types of atoms, see Figs. 8(b)–8(d). The acoustic modes and the optical modes with predominantly Fe contributions are found in the lowest energy region $E<30$ meV [Fig. 8(b)]. They are separated by a narrow gap near $E=31$ meV from the optical

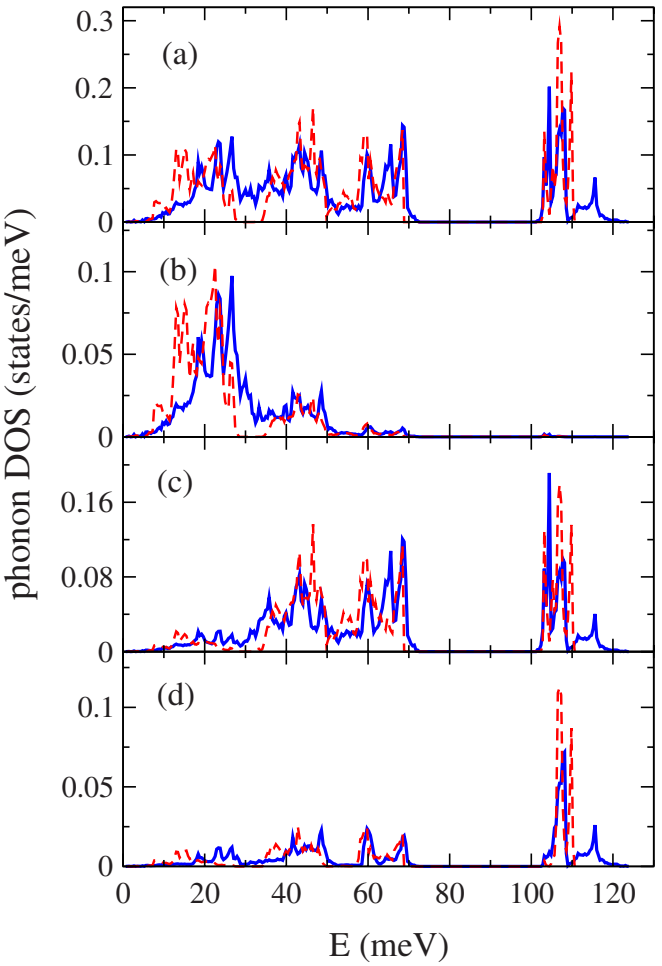

FIG. 8. (Color online) Phonon DOS obtained for the AF structure of Fe_2SiO_4 spinel with $U=0$ eV (dashed lines) and $U=4.5$ eV (full lines): (a) total, (b) partial for iron atoms, (c) partial for oxygen atoms, and (d) partial for silicon atoms.

modes in the intermediate energy region which arise mainly due to oxygen vibrations [Fig. 8(c)]. The largest energy gap, of around 33 meV wide, is found between $E=70$ and 103 meV. It separates the internal Si-O stretching vibrations (above $E=103$ meV) from the rest of the spectrum. They are rather well localized and thus concentrated in a very narrow energy range of about 8 meV wide, in contrast to the dispersive modes of mainly oxygen (31–70 meV) and iron origin (<30 meV). The contribution of silicon atoms to other than the Si-O stretching modes is very small; see Fig. 8(d).

The inclusion of electronic interaction via the realistic value of $U=4.5$ eV causes qualitative changes in the phonon spectrum of Fe_2SiO_4 spinel (Fig. 7, bottom). These differences result from the metal-insulator transition and have two distinct origins. The first of them is related to the LO-TO splitting of the optical IR modes induced by the macroscopic polarization. This effect is clearly seen for the highest optical phonon where the energy of the LO mode increases at the Γ point from 108.7 to 123.7 meV (Fig. 7, bottom). The second effect is connected directly to the local Coulomb interactions U, which modify the charge distribution around Fe ions, thus influencing the interatomic interactions which in turn determine the phonon energies. As expected, the phonon modes with the largest energy changes involve predominantly iron vibrations [Fig. 8(b)]. Due to their significant shift to higher energies, they approach the region of predominantly oxygen vibrations and the energy gap between the two regions vanishes [Figs. 7 (bottom) and 8(a)]. The upward energy shift is not as pronounced for the oxygen vibrations [Fig. 8(c)], since they are only indirectly influenced by Coulomb interactions due to the hybridization between Fe($3d$) and O($2p$) states. As expected, the high-energy modes representing the Si-O stretching vibrations are almost unchanged, except for somewhat increased dispersion resulting in the mode which extends up to $E=125$ meV, which demonstrates the coupling between the Si and Fe atoms via the electronic structure. Finally, comparably small changes as for oxygen vibrations are observed for silicon vibrations [Fig. 8(d)].

TABLE II. Phonon mode degeneracies d and frequencies E (in meV) as obtained at the Γ point of the Brillouin zone for the AF configuration of Fe_2SiO_4 spinel. The results obtained for the uncorrelated electronic structure ($U=0$) are compared with the ones found for realistic on-site Coulomb interaction $U=4.5$ eV. Energies of the LO infrared modes resulting from the LO-TO splitting are given in parentheses.

	Frequency E			
d	$U=0$	$U=4.5$ eV	Symmetry	Activity
3	15.75	26.19(26.46)	T_{1u}	Infrared
3	20.77	20.67	T_{2u}	Silent
1	22.40	39.12	A_{2u}	Silent
2	22.77	29.03	E_u	Silent
3	32.52	26.62	T_{1g}	Silent
3	36.27	43.63	T_{2g}	Raman
3	41.71	42.85(51.19)	T_{1u}	Infrared
2	46.22	27.46	E_g	Raman
3	51.08	52.20	T_{2u}	Silent
3	61.09	62.81(72.36)	T_{1u}	Infrared
2	64.36	66.22	E_u	Silent
3	68.34	68.93	T_{2g}	Raman
1	103.91	104.24	A_{2u}	Silent
3	106.17	108.19	T_{2g}	Raman
1	107.84	101.40	A_{1g}	Raman
3	108.23	108.70(123.66)	T_{1u}	Infrared

In Table II we present a detailed comparison of the phonon frequencies calculated at the Γ point for two values of U: 0 and 4.5 eV. When $U=4.5$ eV, the IR-T_{1u} modes experience the LO-TO splitting, so the energies of the LO components are included in parentheses. Table II shows that majority of the modes shift to higher energies in the Mott insulating state when $3d$ electrons at Fe atoms interact with each other due to finite value of U. The largest energy increase is observed for the lowest T_{1u}, A_{2u}, E_u, and T_{2g} phonon modes, which represent mainly vibrations of Fe atoms. The largest change in phonon energy, $\Delta E=10.4$ meV, was found for the optic mode with the T_{1u} symmetry. Its energy shift due to the metal-insulator transition is much larger than

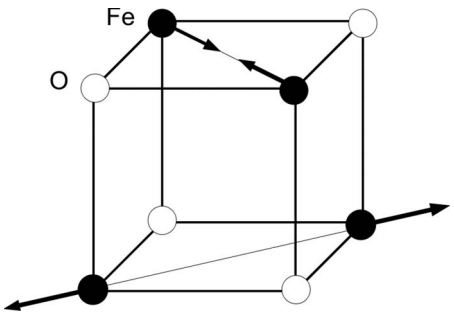

FIG. 9. Schematic Fe atom distortions in the lowest T_{1u} infrared optic mode.

its LO-TO splitting (0.27 meV). As shown in the schematic visualization of the T_{1u} mode (Fig. 9), this phonon involves only Fe distortions along the diagonal [110] direction, modulating directly the Fe-Fe distance. Interestingly, large energy splitting of this very mode was observed in $ZnCr_2O_4$ spinel where it was explained as induced by the AF order below the spin-Peierls transition.[13] The above mentioned facts point toward the universal character of the spin-phonon coupling in transition-metal spinels, and we believe that future experiments will confirm the anomalous behavior of T_{1u} mode in Fe_2SiO_4 spinel.

It is remarkable that the phonon energies increase with U, despite the larger volume V obtained with finite U calculations (Table I), which would suggest the opposite trend. In a typical situation, observed, e.g., in metals, the volume increase for $U>0$ corresponds to larger interatomic distances and consequently to smaller force constants which results in lower phonon energies.[29,34] In contrast to this typical situation, the change in phonon energies in Fe_2SiO_4 spinel is directly related to the metal-insulator transition, which strongly modifies the electronic properties. On one hand, in a metallic state, the interatomic forces are weakened by the charge screening of delocalized electrons. On the other hand, in an insulator, electronic interactions, introduced here by U, result in their localization and induce such charge redistribution which weakens the screening of ionic interactions. Thus, effectively, the strong on-site Coulomb interactions cause strengthening of interatomic forces, which then leads to larger force constants and higher phonon frequencies. Comparing the on-site force constants of Fe, O, and Si atoms obtained for U equal to 0 and 4.5 eV, one finds that Fe force constant increases the most by as much as 24%. For the oxygen atom this increase is only 1.4%, and for the silicon atom the change is negligible. Therefore, the effect of U on the lattice dynamics has a rather local character and the local interactions between $3d$ electrons influence mainly the dynamics of Fe atoms. It is most readily pronounced for the T_{1u} mode, and follows from its local character, as this mode can be described as nearest-neighbor Fe-Fe distance stretching (see Fig. 9). In this mode, the force constant between two nearest-neighbor Fe ions largely depends on Coulomb repulsion, being modified by the electron screening.

IV. COMPARISON WITH MAGNETITE

The electronic and vibrational properties of Fe_2SiO_4 spinel can be compared to those of Fe_3O_4. At room temperature, both these materials crystallize in the cubic ($Fd\bar{3}m$) symmetry and differ only by the type of atom in the tetrahedral position. For $U=0$ eV, their electronic structures are very similar, with the t_{2g}-band states, belonging to the octahedral Fe sites, crossing the Fermi energy. In both cases, the magnetic moments at the octahedral Fe sites are ordered ferromagnetically. In magnetite, however, there are additional moments at the tetrahedron sites with the opposite directions, and thus the resulting magnetic order is ferrimagnetic.

Although the insulating state in both materials is induced by the Hubbard interaction U, two mechanisms of the metal-insulator transition can be distinguished. In Fe_2SiO_4 spinel, even not too high values of $U(U>2$ eV) are sufficient to generate the insulating state with the AF ordering and the gap being proportional to U. Magnetite, in the cubic phase, remains a ferrimagnetic metal even for high values of U. Only when the crystal structure is distorted and its symmetry is lowered, the metal-insulator (Verwey) transition occurs.[14] In this case, the gain in energy comes not only from the gap opening but both the electron localization and crystal distortion are involved. This explains much smaller gap ($\Delta=0.18$ eV) than in Mott insulators. The differences between these two mechanisms result mainly from the electron occupation in the t_{2g} states on Fe atoms at the octahedral sites. While the average number of $3d$ electrons in Fe_2SiO_4 spinel is close to six (Fe^{2+}), which gives effectively one t_{2g} electron at the Fermi level per Fe atom, the average number of t_{2g} electrons in magnetite is reduced to $\sim 5.5(Fe^{2.5+})$. This mixed-valent state in magnetite is the origin of the metallic state at high temperatures and charge-ordering phase below the Verwey transition. In Fe_2SiO_4, the higher electron density and strong Hubbard interaction prohibits the charge fluctuations, so the insulating phase with the uniform charge distribution at Fe sites is stable at all temperatures.

Significant differences between these two materials are found also in their phonon spectra. Due to strong interatomic forces in the SiO_4 tetrahedra, phonon energies in Fe_2SiO_4 spinel reach much higher values (above 123 meV) than in magnetite (81 meV). Additionally, in contrary to magnetite, these high energy vibrations are separated from other modes by the gap of ~ 30 meV wide. In both compounds, phonon energies are strongly influenced by the local interaction U, but the present results show that in Fe_2SiO_4 spinel this effect is largely enhanced by the metal-insulator transition. Therefore, the changes in phonon energies induced by U are larger in Fe_2SiO_4 spinel than in magnetite. While in the case of magnetite, the importance of electron correlations was proved by the comparison with the experimental data,[14] we presume that future neutron or x-ray phonon measurements will demonstrate that the phonon frequencies obtained with finite Coulomb repulsion U are closer to experimental values than the ones obtained with $U=0$, and will thus confirm our prediction that local Coulomb interactions influence the phonon spectra.

V. SUMMARY AND FINAL REMARKS

The main objective of this study was to find the electronic (magnetic) ground state of Fe_2SiO_4 spinel and to understand

the effect of strong electron correlations of the $3d$ electrons at Fe ions on its structural and dynamical properties. We have found that the local electron interactions, included here as the Coulomb on-site energy U and Hund's exchange J_H, strongly determine the magnetic properties of this material. For $U \leq 2$ eV, the metallic state has the FM order, and the system behaves like a typical band (Stoner) ferromagnet. In the range of $2 < U < 3$ eV, the metal-insulator transition occurs, and the magnetic order in the ground state transforms simultaneously from the FM into the AF phase.

As we have discussed, the AF state (unlike the FM one) breaks the cubic symmetry and induces changes in the interatomic distances. Without this distortion, the AF state would have a triple degeneracy and the ground state would be highly frustrated. The existence of geometrically frustrated state in Fe_2SiO_4 spinel is consistent with its very low Néel temperature T_N in comparison to the Curie-Weiss temperature θ_{CW}; Eq. (2). The tetragonal distortion relieves the ground-state degeneracy and removes partly the magnetic frustration in the system. We have found that the distance between the parallel spins increases by about 0.4% and between the antiparallel spins decreases by about 0.3% for the realistic value of Coulomb interaction $U=4.5$ eV. So, this deformation enhances the AF exchange in the four bonds out of six in a single Fe tetrahedron (see Fig. 6). Such a crystal distortion induced by the AF order is typical for the spin-Peierls phase transition observed, e.g., in $ZnCr_2O_4$ spinel. In the case of Fe_2SiO_4 spinel, the theoretical prediction of a similar phase transition discussed here could be verified experimentally provided that detailed crystallographic and magnetic measurements are performed below T_N under high pressure.

The properties of strongly correlated $3d$ electrons in the ground state determine also the phonon spectrum. As we have shown, the changes in phonon energies found for the modes involving Fe atoms are very large (even up to 70%). These changes are mainly associated with the metal-insulator transition which occurs for an intermediate value of $U \sim 2$ eV, well below the realistic value for Fe_2SiO_4 spinel. In addition, lattice dynamics depends also on the spin configuration, indicating a strong spin-phonon coupling in Fe_2SiO_4 spinel.

Independently of the actual value of U, stable phonon spectra have been found only for the AF phase. In case of the metallic state, the FM configuration results in dynamically unstable structure. This result is, however, in conflict with the total energy calculations which suggest that the ground state is characterized by the FM order at $U=0$. We remark that the problem with the stability of FM configuration appears also in the GGA+U calculations, for realistic (and smaller) values of U. While comparable total energies were obtained for both magnetic configurations, the FM structure appears to be electronically unstable under the atomic displacements, prohibiting us from calculating the HF forces. Therefore, we conclude that the stability of the ground state determined by standard methods used to determine the electronic structure is a rather subtle problem in case of materials with strongly correlated electrons, and definite conclusions are possible only by investigating dynamical stability.

Summarizing, we determined the electronic structure and the phonon spectra for the AF phase of Fe_2SiO_4 spinel which is both energetically and dynamically stable in the expected range of on-site Coulomb interactions with $U \sim 4.5$ eV. Therefore, the present results strongly suggest that the Fe_2SiO_4 spinel is the Mott-Hubbard insulator, with the AF order and tetragonally distorted crystal structure which permits symmetry breaking in a system with frustrated antiferromagnetic interactions.

ACKNOWLEDGMENTS

This work was supported in part by Marie Curie Research Training Network under Contract No. MRTN-CT-2006-035957 (c2c) and by the Polish government (MNiSW) within Contract No. 541/6.PR UE/2008/7. A.M.O. acknowledges financial support by the Foundation for Polish Science (FNP) and by the Polish Ministry of Science and Education under Project No. N202 068 32/1481.

*Present address: Interdisciplinary Centre for Mathematical and Computational Modelling (ICM), University of Warsaw, Pawinskiego 5A, PL-02106 Warsaw, Poland.

[1] A. E. Ringwood and A. Major, Earth Planet. Sci. Lett. **1**, 241 (1966).

[2] E. Ohtani and M. Kumazawa, Phys. Earth Planet. Inter. **27**, 32 (1981); Y. Meng, Y. Fei, D. J. Weidner, G. D. Gwanmesia, and J. Hu, Phys. Chem. Miner. **21**, 407 (1994); A. Chopelas, Am. Mineral. **85**, 270 (2000).

[3] P. Piekarz, P. T. Jochym, K. Parlinski, and J. Łażewski, J. Chem. Phys. **117**, 3340 (2002); Y. G. Yu and R. M. Wentzcovitch, J. Geophys. Res. **111**, B12202 (2006).

[4] M. Imada, A. Fujimori, and Y. Tokura, Rev. Mod. Phys. **70**, 1039 (1998).

[5] M. Cococcioni, A. Dal Corso, and S. de Gironcoli, Phys. Rev. B **67**, 094106 (2003).

[6] X. Jiang and G. Y. Guo, Phys. Rev. B **69**, 155108 (2004).

[7] Q. Williams, E. Knittle, R. Reichlin, S. Martin, and R. Jeanloz, J. Geophys. Res. **95**, 21549 (1990).

[8] R. A. Robie, C. B. Finch, and B. S. Hemingway, Am. Mineral. **67**, 463 (1982).

[9] I. Choe, R. Ingalls, J. M. Brown, and Y. Sato-Sorensen, Phys. Chem. Miner. **19**, 236 (1992).

[10] W. Yong, E. Dachs, and A. C. Withers, Phys. Chem. Miner. **34**, 121 (2007).

[11] O. Tchernyshyov, R. Moessner, and S. L. Sondhi, Phys. Rev. Lett. **88**, 067203 (2002).

[12] *Frustrated Spin Systems*, edited by H. T. Diep (World Scientific, Singapore, 2004).

[13] A. B. Sushkov, O. Tchernyshyov, W. Ratcliff II, S. W. Cheong, and H. D. Drew, Phys. Rev. Lett. **94**, 137202 (2005); C. J. Fennie and K. M. Rabe, *ibid.* **96**, 205505 (2006).

[14] P. Piekarz, K. Parlinski, and A. M. Oleś, Phys. Rev. Lett. **97**, 156402 (2006); Phys. Rev. B **76**, 165124 (2007).

[15] L. Pintschovius and M. Braden, Phys. Rev. B **60**, R15039 (1999); R. J. McQueeney, Y. Petrov, T. Egami, M. Yethiraj, G. Shirane, and Y. Endoh, Phys. Rev. Lett. **82**, 628 (1999).
[16] S. Y. Savrasov and G. Kotliar, Phys. Rev. Lett. **90**, 056401 (2003).
[17] P. Zhang, S. G. Louie, and M. L. Cohen, Phys. Rev. Lett. **98**, 067005 (2007).
[18] U. D. Wdowik and K. Parlinski, Phys. Rev. B **75**, 104306 (2007).
[19] M. Zbiri, T. Fennell, J. W. Taylor, M. Enderle, G. C. Lau, R. J. Cava, and M. R. Johnson, J. Phys.: Condens. Matter **20**, 285203 (2008).
[20] G. Kresse and J. Furthmüller, Comput. Mater. Sci. **6**, 15 (1996); Phys. Rev. B **54**, 11169 (1996).
[21] J. P. Perdew, K. Burke, and M. Ernzerhof, Phys. Rev. Lett. **77**, 3865 (1996).
[22] A. M. Oleś, Phys. Rev. B **28**, 327 (1983); A. M. Oleś, G. Khaliullin, P. Horsch, and L. F. Feiner, *ibid.* **72**, 214431 (2005).
[23] J. Zaanen and G. A. Sawatzky, J. Solid State Chem. **88**, 8 (1990).
[24] K. Parlinski, Z. Q. Li, and Y. Kawazoe, Phys. Rev. Lett. **78**, 4063 (1997).
[25] K. Parlinski, Software PHONON, Cracow, 2008.
[26] R. Pick, M. H. Cohen, and R. M. Martin, Phys. Rev. B **1**, 910 (1970).
[27] H. Suto, C. Koike, H. Sogawa, A. Tsuchiyama, H. Chihara, and K. Mizutani, Astron. Astrophys. **389**, 568 (2002).
[28] T. Yagi, F. Marumo, and S. I. Akimoto, Am. Mineral. **59**, 486 (1974).
[29] P. Piekarz, K. Parlinski, P. T. Jochym, A. M. Oleś, J. P. Sanchez, and J. Rebizant, Phys. Rev. B **72**, 014521 (2005).
[30] J. Zaanen, G. A. Sawatzky, and J. W. Allen, Phys. Rev. Lett. **55**, 418 (1985).
[31] H. K. Mao and M. P. Bell, Science **176**, 403 (1972).
[32] Q. Williams, E. Knittle, R. Reichlin, S. Martin, and R. Jeanloz, J. Geophys. Res. **95**, 21549 (1990).
[33] A. M. Oleś and G. Stollhoff, Phys. Rev. B **29**, 314 (1984); G. Stollhoff, A. M. Oleś, and V. Heine, *ibid.* **41**, 7028 (1990); Phys. Rev. Lett. **76**, 855 (1996).
[34] J. Łażewski, P. Piekarz, A. M. Oleś, and K. Parlinski, Phys. Rev. B **74**, 174304 (2006).